EGFR/uPAR interaction as druggable target to overcome vemurafenib acquired resistance in melanoma cells

Anna Laurenzana [a,*], Francesca Margheri [a], Alessio Biagioni [a], Anastasia Chillà [a], Nicola Pimpinelli [b], Jessica Ruzzolini [a], Silvia Peppicelli [a], Elena Andreucci [a], Lido Calorini [a], Simona Serratì [c], Mario Del Rosso [a,*], Gabriella Fibbi [a]

[a] Department of Experimental and Clinical Biomedical Sciences "Mario Serio", University of Florence, Viale G.B. Morgagni, 50, 50134 Florence, Italy
[b] Dermatology Unit, Department of Surgery and Translational Medicine, University of Florence, Viale Michelangiolo, 41, 50125 Florence, Italy
[c] Nanotecnology Laboratory, National Cancer Research Centre, IRCCS "Giovanni Paolo II", Viale Orazio Flacco, 65, 70124 Bari, Italy

ARTICLE INFO

ABSTRACT

Background: BRAF inhibitor (BRAF-I) therapy for melanoma patients harboring the V600E mutation is initially highly effective, but almost all patients relapse within a few months. Understanding the molecular mechanisms behind BRAF-I responsiveness and acquired resistance is therefore an important issue. Here we assessed the role of urokinase type plasminogen activator receptor (uPAR) as a potentially valuable biomarker in the acquisition of BRAF-I resistance in V600E mutant melanoma cells.
Methods: We examined uPAR and EGFR levels by real time PCR and western blot analysis. uPAR loss of function was realized by knocking down uPAR by RNAi or using M25, a peptide that uncouples uPAR-integrin interaction. We investigated uPAR-β1integrin-EGFR association by co-immunoprecipitation and confocal immuno-fluorescence analysis. Acquired resistance to BRAF-I was generated by chronic exposure of cells to vemurafenib.
Findings: We proved that uPAR knockdown in combination with vemurafenib inhibits melanoma cell proliferation to greater extent than either treatment alone causing a decrease in AKT and ERK1/2 phosphorylation. Conversely, we demonstrated that uPAR enforced over-expression results in reduced sensitivity to BRAF inhibition. Moreover, by targeting uPAR and EGFR interaction with an integrin antagonist peptide we restored vemurafenib responsiveness in melanoma resistant cells. Furthermore, we found significant detectable uPAR and EGFR levels in tumor biopsies of 4 relapsed patients.
Interpretation: We disclosed an unpredicted mechanism of reduced sensitiveness to BRAF inhibition, driven by elevated levels of uPAR and identified a potential therapeutic strategy to overcome acquired resistance.
Funds: Associazione Italiana Ricerca sul Cancro (AIRC); Ente Cassa di Risparmio di Firenze.

1. Introduction

Metastatic melanomas are the deadliest form of skin cancer and have the highest mutational loads of all cancers [1]. Until recently, effective treatments for surgically unresectable or metastatic melanoma were lacking. At the most, cytotoxic chemotherapy such as dacarbazine or immunotherapies with interleukin-2 (IL-2) for instance, yield response rate of approximately 10%. Even though these responses may be extremely durable, neither aforementioned treatments results in improved overall survival (OS) [2–4].

Encouraging perspectives for patients with advanced melanoma significantly arose with the identification of specific BRAF and MEK inhibitors and immune modulating antibodies [5] as effective therapies. BRAF is a serine–threonine-specific protein kinase, belonging to the RAF family (RAF1, ARAF, and BRAF) of kinases, that act downstream of RAS and upstream of MEK in the MAPK signaling pathways, mediating cell proliferation in response to several growth signals under normal signaling conditions. Dysregulation of the MAPK pathway is a key feature in the majority of melanomas. Indeed, about 28% of melanomas contain activating mutations in NRAS [6,7], whereas approximately 52% of all melanomas contain a mutation in the BRAF gene, most commonly resulting in substitution of valine for glutamic acid at position 600 (V600E) [8,9]. The BRAFV600E substitution leads to constitutive activation of this kinase and, consequently, of constitutive ERK signaling. Inhibition of the BRAF (V600E) oncoprotein by the small-molecule drug

* Corresponding authors.
E-mail addresses: anna.laurenzana@unifi.it (A. Laurenzana), delrosso@unifi.it (M. Del Rosso).

Research in context

Evidence before the study

Oncogenic mutations in the *BRAF* gene, that cause the protein to become overactive, are present in about 7% of human cancers and in about 50% of advanced (unresectable or metastatic) melanomas. *BRAF* mutation status is the only biomarker that predicts a therapeutic response in advanced melanoma, making possible to treat melanoma patients with inhibitors of mutated *BRAF* (BRAF-I, such as vemurafenib). Unfortunately, patients relapse within 6—8 months from the beginning of therapy due to the development of different mechanisms of acquired tumor drug resistance. The capability to by-pass the inhibitor effect can be achieved through different mechanisms: emergence of *BRAF* alternative gene expression variants, mutations in the mitogen cascade (MAPK pathway), or activation of alternative cell survival signals (PI3k/AKT/mTOR pathway).

Added value of this study

In the present study we showed that among the several molecular effectors involved in BRAF resistance to vemurafenib, the urokinase plasminogen activator receptor (uPAR) plays a crucial role. Indeed, we demonstrated that cells with different uPAR expression levels display variable sensitivity to the BRAF-I. More importantly, we proved that resistance to Vemurafenib depends on uPAR-EGFR interaction, and identified a potential therapeutic strategy to inhibit this interaction by using a small peptide able to dissociate uPAR and EGFR. Such dissociation inhibits the resistance-associated PI3k/AKT/mTOR pathway and leaves the MAPK pathway, sensitive to vemurafenib, as the only signaling pathway.

Implication of all the available evidence

Our data suggest that uPAR may be a useful biomarker to identify patients with BRAF-mutant melanoma who will (low uPAR levels) or will not (high uPAR levels) respond to BRAF inhibitors. Indeeed, the evaluation of uPAR expression levels on V600E mutant patient might improve drug combination design that will lead to more potent, durable personalized therapy. Last, treatment with the small peptide used in this work, may have the chance to restore vemurafenib sensitivity in relapsed patients.

growth factors, extracellular matrix degradation and tumor neo-angiogenesis [16–19]. Several malignant tumors show a positive correlation between uPAR levels and a more aggressive phenotype together with a poor prognosis. uPAR is able to regulate multiple signaling events stimulating several growth factor receptors independently of the presence of the specific cognate ligands [20]. Indeed, $\alpha5\beta1$, $\alpha3\beta1$, $\alpha v\beta3$ and $\alpha v\beta5$ integrins through their alpha chain interact with uPAR in a RGD-independent fashion and with receptor tyrosine kinases (RTK) such as EGFR [21–23], PDGFR, G-protein coupled receptors (GPCR) and MET [24–26]. uPAR-associated growth factor receptors signal through a ligand-independent uPAR/integrin fashion, activating the main transduction pathway, namely the PI3K/AKT/mTOR, that is also activated at the onset of vemurafenib resistance in tumors harboring the BRAF V600E mutation [27].

In this study we provide for the first time in vitro evidence that uPAR levels in BRAF mutant melanoma cells are a key element of response to BRAF inhibition. Indeed, we demonstrated that cells with different uPAR expression levels show variable sensitivity to Vemurafenib. uPAR silencing through RNA interference in A375-M6 metastatic melanoma cells expressing high uPAR levels, restored sensitivity to vemurafenib and induced a more pronounced down-regulation of ERK signaling. Conversely, we proved that uPAR over-expression in cells with moderate uPAR levels results in reduced sensitivity to BRAF inhibition. In addition we cultured BRAF-mutant A375M6 cells in the presence of Vemurafenib until the emergence of resistant derivative and describe a promising combinatorial strategy to address acquired resistance to monotherapy.

Lastly, we retrospectively assessed the impact of EGFR or uPAR expression levels on clinical outcomes in 6 patients with metastatic melanoma treated with vemurafenib. We found significant detectable uPAR and EGFR levels in 4 relapsed patients and two of them exhibited very high levels of mRNA relative to both markers. Our data suggest that uPAR may be a useful biomarker to identify patients with BRAF-mutant melanoma who will or will not respond to BRAF inhibitors (BRAF-I).

2. Materials and methods

2.1. Cell lines and culture conditions

The human melanoma cell lines CRL-1619 A375 (MITF wild type, BRAF V600E, NRAS wild type)were obtained from American Type Culture Collection (Manassas, VA) and were grown in Dulbecco's Modified Eagle Medium high glucose (DMEM 4500, EuroClone, MI, Italy) containing 2 mM glutamine and supplemented with 10% FBS (Euroclone, Milano, Italy). A375-M6 melanoma cells (M6) were isolated in our laboratory from lung metastasis of SCID bg/bg mice i.v. injected with A375 cells. A375, and M6 were independently validated by STR profiling by the DNA diagnostic center BMRGenomics (Padova, Italy). Cells were amplified, stocked, and once thawed were kept in culture for a maximum of 4 months.

In some experiments we used also the human melanoma cell lines WM266-4 (from ATCC), M14, M20, Mewo, W1361A. Melanoma cells were cultivated in DMEM supplemented with 10% fetal bovine serum (FBS) at 37 °C in humidified atmosphere containing 90% air and 10% CO_2. Cells were harvested from subconfluent cultures by incubation with a trypsin-EDTA solution (EuroClone, MI, Italy), and propagated every four days. Viability of the cells was determined by trypan blue exclusion test. Cultures were periodically monitored for mycoplasma contamination using Chen's fluorochrome test.

2.2. Generation of vemurafenib-resistant population

M6 cells were plated at low density (5×10^4) on 10 cm dishes and 24 h later they were treated with 2 μM vemurafenib. Once the cells gained the ability to grow in the presence of vemurafenib (PLX4032, MedChemtronica AB, Stockholm, Sweden), which happened about

PLX4032 also known as Vemurafenib, is effective in the personalized treatment of tumors harboring the BRAF (V600E) mutation [10], especially in melanoma patients. However emergence of acquired drug resistance based on the recovery of constitutive reactivation of MAPK signaling by secondary mutations in NRAS and MEK [11,12] or on activation of alternative signaling pathways by relevant growth factor receptors [13,14], or on the emergence of BRAF alternative splicing isoforms [15], limits clinical benefit. Thus, effective therapies that address both de novo and acquired resistance to BRAF and MEK inhibitors remain a subject of active research. Understanding the mechanisms underlying resistance to vemurafenib, its analogs, or dabrafenib, provides an important basis for developing rational strategies to treat patients with BRAFV600- mutated melanoma who do not respond to BRAF inhibitors, or to treat patients who progress on these therapies.

Among the several molecular effectors involved in drug resistance and, in particular, in BRAF resistance to vemurafenib, the urokinase plasminogen activator receptor (uPAR) might play a crucial role in view of its involvement in intracellular signaling, activation of latent

three months from the beginning of the treatment, they were expanded and analyzed by molecular and cellular assays.

2.3. Cell treatments with M25, MEK1/2, ERK1/2 specific inhibitors

Inhibition of uPAR-integrin interaction was obtained with the M25 peptide, previously identified in a phage display library, able to uncouple uPAR from integrin α-chain. The peptide was produced in collaboration with the Peptide Facility at Biotechnology Center, University of Padova (CRIBI). In the β-propeller model of α-chain folding, the sequence of this peptide (STYHHLSLGYMYTLN) spans an exposed loop on the ligand-binding surface of α-chain, thus impairing integrin α chain-uPAR interaction. In cell culture M25 water solution was used at 50 μM at 37 °C. MEK1/2 inhibition was achieved with 1 μM CI-1040 (Cayman Chemical) while ERK1/2 inhibition was obtained with 1 μM SCH772984 (Cayman Chemical).

2.4. Cell viability determination

The viability of A375 and A375-M6 cells was determined by trypan blue staining. Cells (1.5×10^5) were seeded in 6-well plates and allowed to attach overnight. On the next day cells were treated with Vemurafenib at the indicated concentrations. 96 h later 20 μL of cell suspension were aseptically transferred to a 1.5 mL clear Eppendorf tube and incubated for 3 min at room temperature with an equal volume of 0.4% (w/v) trypan blue solution prepared in 0.81% NaCl and 0.06% (w/v) dibasic potassium phosphate. Viable and nonviable cells (trypan blue positive) were counted separately using a dual-chamber hemocytometer and a light microscope. The means of three independent cell counts were pooled for analysis.

2.5. Clonogenic assay

Cells were seeded (8×10^2) in six well plates and treated with vehicle (DMSO) or different doses of vemurafenib. After 10 days, cells were fixed and stained with MayGrunwald-Giemsa. The number of colonies were counted and reported in graphs.

2.6. Tumor spheroid formation

Tumor cell monolayers were washed with PBS and then harvested using Trypsin, collected and centrifuged at 500 x g for 5 min. 500 cells/well were seeded dispensing 500 μL per well into a 24-well flat-bottomed plate precoated with 1.5% Agar. The plate was then transferred to an incubator (37 °C, 5% CO₂, 95% humidity). Four days later, after the tumor spheroids formation was visually confirmed, the 3D tumor colonies were treated with vemurafenib, M25 peptide or combination (vemurafenib+M25) for one additional week. Images were collected and analyzed by ImageJ software (developed by Wayne Rasband, National Institutes of Health, Bethesda, MD; available at http://rsbweb.nih.gov/ij/index.html). Estimated area was measured after drawing a yellow circle around the selected spheroid.

2.7. Spheroid-based migration assay

500 cells were resuspended in 150 μL of media and plated on an agarose base (PBS plus 1.5% agarose) in 96 well plate. Four days later tumor spheroids formation was visually confirmed, cells were treated with either DMSO or 2uM vemurafenib or M25 or combination and 50 ul of Matrigel (BD Biosciences) (125 μg/mL) were dispensed into the inner wells. Each experimental condition was plated in triplicate. After 3 days, images were collected and analyzed by ImageJ software. The invasive ability was evaluated by measuring the total area outside the spheroid. Invasive area are first defined using the software draw tool, after which comparative values are generated as pixel measurements.

2.8. RNA extraction, semiquantitative and quantitative PCR

Total RNA was prepared using Tri Reagent (Sigma-Aldrich, Saint Louis, Missouri, USA), agarose gelchecked for integrity, and reverse transcribed with cDNA sintesys kit (BioRad, Milano, Italy) according to manufacturer's instructions. Selected genes were evaluated by qualitative PCR using Blue Platinum PCR Super Mix (Life Technologies, Monza, Italy) or Real-Time PCR using SsoAdvanced Universal Green Mix (BioRad, Milano, Italy) with 7500 Fast Real Time PCR System (Applied Biosystems, Waltham, Massachusetts, USA). For Real Time PCR, fold change was determined by the comparative Ct method using β2-Microglobulin as the normalization gene. Amplification was performed with the default PCR setting: 40 cycles of 95 °C for 10 s and of 60 °C for 30 s using SYBR Green–based detection. Primer sequences (IDT, TemaRicerca, Bologna, Italy) were as follows:

18S-rRNA: sense, 5′-CCAGTAAGTGCGGGTCATAAG-3′; antisense, 5′-GCCTCACATAA-CCATCCAATC-3′.

uPAR: sense, 5′-GCCCAATCCTGGAGCTTGA-3; antisense, 5′- TCCCCT TGCAGCTGTA-ACACT-3′.

EGFR sense 5′-GGTGCGAATGACAGTAGCATTATGA-3′; EGFR antisense, 5′-AAAGGTGGGCTCCTAACT-AGCTGAA-3′.

2.9. Western blot analysis

Harvested cells were resuspended in 20 mM RIPA buffer (pH 7.4) (Merk Millipore, Vimodrone, MI, Italy) containing a cocktail of proteinase inhibitors (Calbiochem, Merck, Darmstadt, Germany) and treated by sonication 19(Microson XL-2000, Minisonix, Farmingdale, NY, USA).

Aliquots of supernatants containing equal amounts of protein (30 μg) in Laemmli buffer were separated on Bolt® Bis-Tris Plus gels 4–12% precast polyacrylamide gels (Life Technologies, Monza, Italy). Fractionated proteins were transferred from the gel to a PVDF nitrocellulose membrane using iBlot 2 system (Life Technologies, Monza, Italy). Blots were stained with Ponceau red to ensure equal loading and complete transfer of proteins, then they were blocked for 1 h, at room temperature, with 5% milk in PBS 0.1% tween solution. Subsequently, the membrane were probed at 4 °C overnight with the following primary antibodies: rabbit anti-pAKT (1:1000, Cell signaling Technology, Cat# 9271), rabbit anti AKT (1:1000, Cell signaling Technology, Cat# 4691), rabbit anti-pERK1/2 (1:1000, Cell signaling Technology, Cat# 9101), mouse anti-ERK1/2 (1:1000, St Cruz Biotechnology, Cat# sc-514,302), rabbit anti-pmTOR (Ser2448) (1:1000 Cell signaling Technology, Cat# 2971) and rabbit anti-mTOR (1:1000 Abcam Cat# ab2732); rabbit anti-uPAR (1:500 FL 290, Santa Cruz Biotechnology, Cat# sc-10,815); rabbit anti-EGFR (1:500, Santa Cruz Biotechnology, Cat# sc-03), rabbit GAPDH antibody (1:1000, Cell signaling Technology, Cat# 2118) or mouse anti-α-tubulin monoclonal antibody (1:2000, Sigma, Cat #T6199) were used to assess equal amount of protein loaded in each lane. Anti-Rabbit IgG (whole molecule)–Peroxidase antibody (Sigma, Cat#A0545) or anti-Mouse IgG (whole molecule)–Peroxidase antibody (Sigma, Cat#A9044)have been used as secondary antibodies; the ECL procedure was employed for development.

2.10. uPAR gene silencing and uPAR gene overexpression

Targeting and not-targeting siRNAs were obtained from Dharmacon (Carlo Erba Reagents, Milan, Italy). Specific silencing of uPAR and EGFR genes were performed by transfection of M6 and A375 with small-interfering-RNA (siGENOME SMARTpool, according to the manufactures's instruction). To favour cell internalization siRNAs were incorporated into cationic liposomes, utilizing DharmaFECT transfection reagent. Cells were incubated with transfection mix (24–48 h for mRNA analysis and 48 h for protein and phenotypic analysis, respectively). A375 and M6 were subjected to uPAR overexpression transiently transfecting these cell lines with the pQ2 plasmid which was

obtained with the Okayama-Berg method and containing uPAR under control of a strong promoter.

2.11. Cell cycle analysis

Cell cycle distribution was analyzed by the DNA content using propidium iodide (PI) staining method. Cells were centrifugate and stained with a mixture of 50 μg/ml PI (Sigma-Aldrich, St. Louis, Missouri), 0.1% trisodium citrate and 0.1% NP40 (or triton x-100) in the dark at 4 °C for 30 min. The stained cells were analyzed by flow cytometry (BD-FACS Canto) using red propidium-DNA fluorescence.

2.12. Confocal microscopy analysis

Cells were grown on glass coverslips, washed twice with 1 ml of PBS, fixed for 20 min in 3.7% paraformaldehyde in PBS and permeabilized with 0.1% Triton X-100 in PBS for 5 min. The cells were incubated in blocking buffer (3% BSA and 0.1% Triton X-100 in PBS) for 1 h at room temperature and then stained with the appropriate antibody overnight at 4 °C: mouse anti-uPAR (1:200, Thermo Fisher Scientific, Cat#Mon R-4-02), rabbit anti-Integrin α5β1(Biocomapare, Cat# NBP2-52680) and goat anti-EGFR (Santa Cruz Biotechnology, Cat# sc-31155). Successively, the cells were incubated at room temperature for 1 h with the specific secondary antibody: CY3-conjugated anti-mouse IgG (1:800; Sigma-Aldrich, Cat# C2181), FITC-conjugated anti-rabbit IgG (1:800; Sigma-Aldrich, Cat# F-4151) and Anti-Goat IgG (whole molecule)-FITC (1:800; Sigma-Aldrich, Cat# F7367). Nuclei were stained with the fluorescent Hoechst 33342 dye (DAPI) (10 μg/ml) (Invitrogen) for 15 min at RT. The coverslips containing the labelled cells were mounted with an anti-fade mounting medium (Biomeda, Foster City, CA) and observed under a Bio-Rad MRC 1024 ES Confocal Laser Scanning Microscope (Bio-Rad, Hercules, CA) equipped with a 15 mW Krypton/Argon laser source for fluorescence measurements. The cells were examined with a Nikon Plan Apo X60-oil immersion objective using an excitation wavelength appropriate for Alexa 488 (495 nm). Series of optical sections (XY: 512 × 512 pixels) were then taken through the depth of the cells with a thickness of 1 μm at intervals of 0.8 μm (Z step). A single composite image was obtained by superimposition of twenty optical sections for each sample observed. The collected images were analyzed by ImageJ software.

2.13. Immunoprecipitation and western blot

Protein concentration was determined using Bradford's method and 500 μg of total proteins were incubated with mouse monoclonal uPAR antibody (Thermo Fisher Scientific, Cat#MON R-5-02) or with non-specific IgG (Mouse IgG isotype control, Thermo Fisher Scientific, Cat# 10400C) used as negative control with gentle rocking for 3 h at room temperature followed by incubation with dynabeads protein G (Novex, Life Technologies, Waltham, MA USA) overnight at 4 °C, according to the manufacturer's instructions.The day after the beads were washed six times with lysis buffer, boiled for 5 min in SDS-loading buffer and subjected to SDS–PAGE and western blot. Nitrocellulose membranes were blocked and then probed overnight at 4 °C, with the polyclonal anti-uPAR (1:500 FL 290 Santa Cruz Biotechnology, Cat# sc-10,815); the anti-α5β1 integrin (1:500, Millipore, Cat# MAB2514) and the polyclonal EGFR (rabbit, Santa Cruz Biotechnology, Cat# sc-03). Then, the membranes were rinsed, incubated with peroxidase-conjugated anti-rabbit immunoglobulin G (1 h, room temperature). After extensive washes, the reaction was revealed using the detection system from GE Healthcare (Milano, Italy the Super Signal West).

2.14. Clinical samples

Clinical samples were collected from 6 melanoma patients at the Plastic and Reconstructive Surgery Unit, Regional Melanoma Referral Center and Melanoma & Skin Cancer Unit, Florence, Italy, after obtaining informed written consent. The study was conducted according to the 1964 Helsinki declaration and Local Institutional Ethics Committee approval. The main characteristics of the patients, their clinical responses according to the classical RECIST1.1 [28] evaluation criteria, and the histological variables such as Breslow thickness (mm), melanoma subtypes, stage, presence of ulceration, mitotic rate (n./mm^2) are reported in Fig. 6.

2.15. Formalin-fixed paraffin-embedded (FFPE) RNA extraction sample and quantitative RT-PCR (qRT-PCR)

Eight to ten 10 μm-thick sections were cut from each block of FFPE tissue, transferred to 1.5-ml sterile tubes, and processed using the PureLink FFPE Total RNA Isolation Kit (Invitrogen, by Thermofisher) according to the manufacturer's protocol. Briefly, RNA was extracted by spin column purification according to similar basic principles: deparaffinization, followed by cell disruption with heated proteinase K, which is capable of efficiently degrading proteins that were covalently cross-linked with each other and RNA. Proteinase K incubation at high temperature (60 to 70 °C) also removes part of the methylol additions induced by formalin fixation [29]. After proteinase K incubation, RNA was isolated by alcohol precipitation in a spin column purification step and then was stored at −80 °C. Total RNA 260/280 OD ratios were consistently between 1.7 and 1.85, indicating high sample purity.

500 ng RNA was reverse-transcribed using Thermo Scientific Maxima H Minus cDNA Synthesis Master Mix with dsDNase (Invitrogen, by Thermofisher) according to manufacturer's instructions. cDNA was amplified (50 °C, 2 min, 95 °C, 10 min, 95 °C, 15 s, 60 °C, 1 min, 50×), and ΔCt was determined using TaqMan Gene Expression duplex assay specific for PLAUR (FAM-MGB, Minor Groove binder, Applied Biosystem) and Glyceraldehyde-3-phosphate dehydrogenase (*GAPDH*) (VIC-MGB primer limited), employed as reference transcript, on the 7500 Applied Biosystem Real-Time PCR System. Similar protocols were obtained to quantify uPAR and EGFR expression levels using a SYBR Green–based detection method (Applied Biosystems).

2.16. Statistical analysis

Data were analyzed using GraphPad Prism 6 and expressed as mean ± SD. The statistical tests used are stated in the Figure legends. A p value of <0.05 was considered significant.

3. Results

3.1. EGFR and uPAR levels in melanoma cells

Given the notion that EGFR levels determine the response to BRAF inhibitor monotherapy [30] and taking in consideration the strong engagement between EGFR and uPAR in melanoma cells [31],we compared EGFR and uPAR protein levels in a panel of wild type and BRAF (V600E) mutant melanoma cell lines (Fig. 1a). Melanoma cells indeed express low or moderate levels of EGFR and uPAR: of the seven melanoma cell lines examined only three, namely W1361A (BRAF wt), A375 e M6 (BRAF V600E), express much higher levels of EGFR and uPAR (Fig. 1b) and constitutive activation of ERK occurred only in two out of 7 cell lines. In order to establish a potential direct correlation between EGFR and uPAR levels, we ablated uPAR in M6 overexpressing cells with specific siRNA smart pools (siPLAUR) for 48 h that efficiently down regulated uPAR expression (Fig. 1c) while induced a slight increase of EGFR expression (Fig. 1d) and protein levels (Fig. 1e) as assessed by PCR and immunoblotting. Furthermore, the inverse experiment of EGFR silencing did not result in any significant effect on uPAR expression (Fig. 1e) and protein levels (Fig. 1f). As EGFR did not cause any change in uPAR protein expression, we continued to investigate the effect of uPAR overexpression in A375 cells on EGFR gene
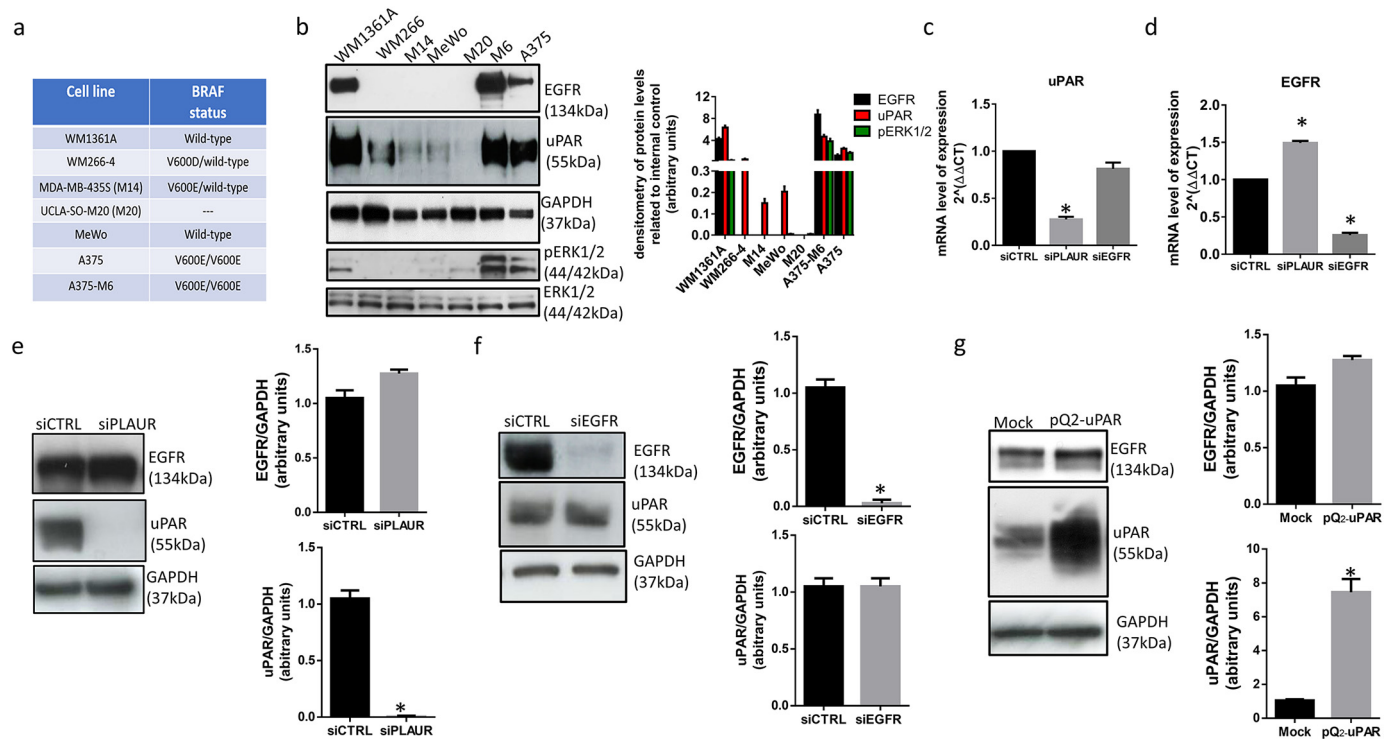
Fig. 1. uPAR, EGFR expression level association in melanoma cells. a. List of melanoma cell lines evaluated for uPAR, EGFR and pERK1/2 protein levels. b. Western blot analysis of EGFR, uPAR and phosphorylation ERK1/2 levels with related densitometric quantification normalized to the internal control. Numbers on the right refer to molecular weights expressed in kDa. c, d. Real time PCR analysis was performed in M6 cells transfected with specific uPAR or EGFR siRNAs and no targeting siRNA as Control, to evaluate the expression levels of uPAR and EGFR. Results of three independent experiments performed in triplicates are expressed as fold changeaccording to $2^{-\Delta\Delta CT}$ method, using 18S as calibrator. Statistical analysis was performed using unpaired Student's t-test, Error bars: mean $\pm$ SD; *p < .05 compared to Control. e, f. Cellular extracts of M6 before and after gene silencing were immunoblotted with antibodies against uPAR and EGFR. GAPDH was included as a loading control. Relative protein levels of uPAR and EGFR were quantified by densitometry and reported as values normalized to the GAPDH. Statistical analysis was performed using unpaired Student's t-test, Error bars: mean $\pm$ SD; *p < .05 compared to Control. g. Cellular extracts of A375 before and after enforced expression with pQ2-uPAR plasmid were analyzed with antibodies against uPAR and EGFR. GAPDH used as a loading control. Densitometric analysis of the levels of the same proteins relative to GAPDH expression. Error bars indicate mean $\pm$ SD; n = 3 experiments; Statistical analysis was performed using unpaired Student's t-test, Error bars: mean $\pm$ SD; *p < .05 compared to Mock Control.

expression. We found that uPAR overexpression in A375 with relatively low endogenous expression levels did not modify EGFR levels compared with the same cells transfected with the empty vector (Fig. 1g), thereby concluding that no mono-directional or mutual regulation of expression is appreciable between uPAR and EGFR in melanoma cells.

### 3.2. Correlation between EGFR levels and uPAR levels and response to BRAF inhibition in melanoma

Given the observation that uPAR and EGFR are differentially expressed in A375 cell line and in its highly metastatic derivative M6, (Fig. 2a, Fig. 2b), we tested the two cell lines for their response to Vemurafenib in short term and long term cultures (Fig. 2c, Fig. S1 and 2d). For the short term assay, cells were treated with increasing concentrations of vemurafenib for 96 h, and cell viability was determined by Trypan blue assay, while for the long term assay cells were grown in the absence or presence of vemurafenib at the indicated concentrations for 10 days. For each cell line, all dishes were fixed at the same time, stained and photographed. As reported in Fig. 2c, in both cell lines the treatment promoted at each dose a flat and elongated morphology and reduced cell proliferation. However, M6 cells seemed to be less responsive than A375 cells to vemurafenib-mediated cytostasis as shown by the fact that a similar growth inhibition in the two cell lines was obtained only by treating M6 cells with a dosage five times higher (5 μM) in the short term assay and 10 times higher in the long term assays than that employed for A375 cells (Fig. 2d). Since the major molecular effect of vemurafenib is inhibition of the MAPK signaling pathway, with a strong reduction of ERK phosphorylation, leading to downstream suppression of cyclin D1 we confirmed its activity evaluating the

phosphorylation levels of ERK (Fig. 2e), the expression (Fig. 2f) and protein levels of Cyclin D1 (Fig. 2g) by Western blot and real time PCR in M6 and A375 cells after 48 h treatment. As shown in figure, both cell lines responded to treatment with 0.5 μM vemurafenib that dramatically reduced the phosphorylation of ERK1/2, and expression and protein levels of Cyclin D1.

Notably, these results showed that the sensitivity of melanoma along with both short-term (Fig. 2c) and long-term (Fig. 2d) proliferation assays and western blot analysis mirrors the expression levels of EGFR and uPAR (Fig. 2b), withA375 being more sensitive to Vemurafenib than M6 cells.

3.3. uPAR overexpression prevents the sensitivity of melanoma cells to vemurafenib

To elucidate the role of uPAR in vemurafenib responsiveness, separate ablation and overexpression experiments were performed using either siRNA-PLAUR or pQ2-DNAuPAR in M6 and A375 cells respectively. We depleted uPAR by transfecting siRNA-PLAUR into M6 cells and then subjected the cells to treatment with increasing concentrations of Vemurafenib. We found that siRNA-mediated depletion of uPAR strongly reduced the colony number compared to control siRNA (siCTRL) treated cells (Fig. 3a) and powerfully enhanced the sensitivity to vemurafenib. Indeed, the number of total colonies decreased in a dose dependent manner and even the lowest vemurafenib dose significantly diminished colony size and number. Moreover, long term proliferation assay after uPAR silencing in A375 (Fig. S2 a, b) in presence of increasing concentrations of vemurafenib substantiated the above results confirming the direct involvement of uPAR in vemurafenib sensitivity.
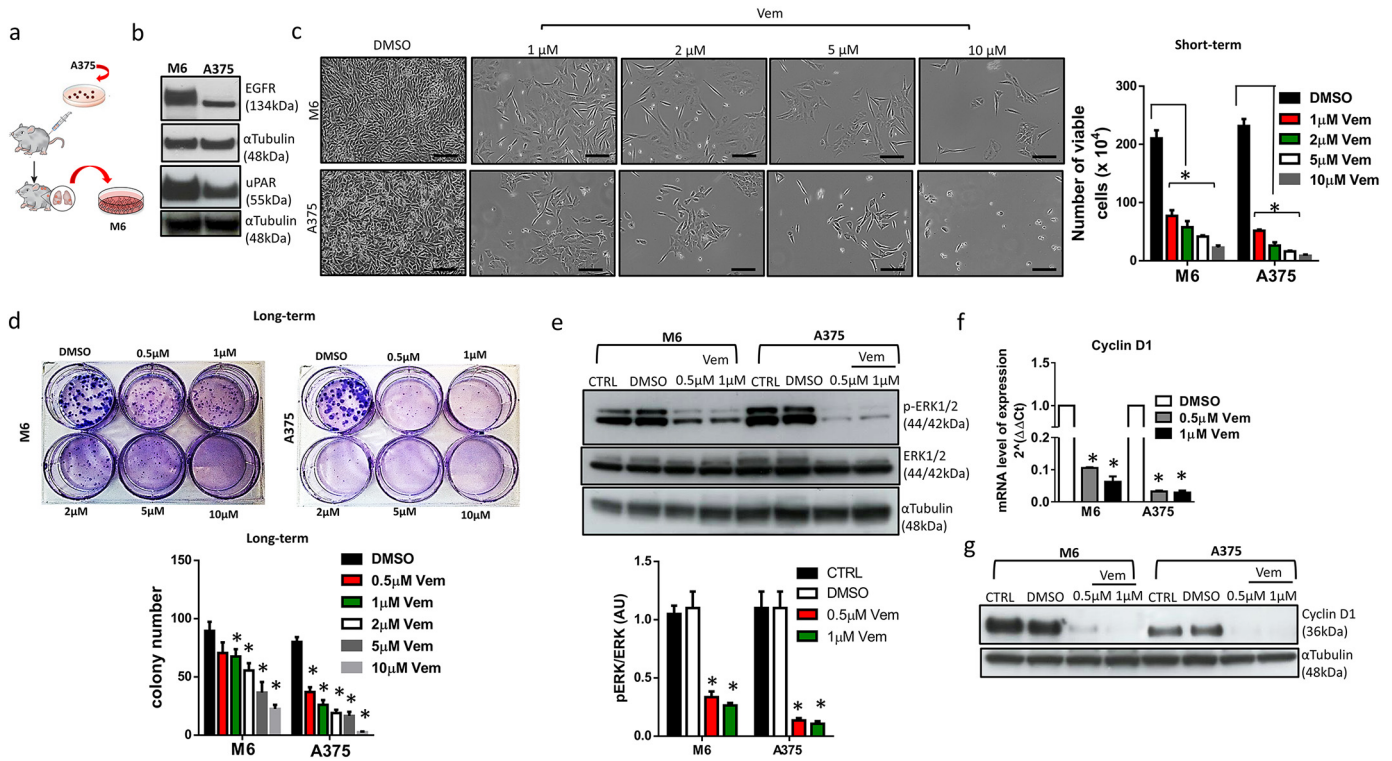
Fig. 2. uPAR levels and responsiveness to BRAF inhibitor in A375 and M6 melanoma cells. a. Schematic representation of M6 generation. b. Immunoblotting for uPAR and EGFR in A375 and M6, αTubulin used as internal control.c. M6 and A375 were treated for 96 h with increasing concentrations of vemurafenib. DMSO-treated cells were set as the control vehicle. Pictures of treated cultures were taken with a phase-contrast microscopy (on the left), viable cells (trypan blu-negative) were counted with the aid of a Burker (on the right). Scale bar = 50 μm. Statistical analysis was performed using unpaired Student's t-test, Error bars: mean ± SD; *p < .05 indicate significant differencefrom DMSO. d. Clonogenic assay of M6 and A375 cellsafter a 10 d-treatment with the indicated doses of BRAF-I. Colonies were stained with May Grunwald and then counted. Statistical analysis was performed using student t-test. Representative data of three independent experiments is shown (mean ± SD). Asterisks indicate significant differences (P < .05.) from DMSO-treated cells. e. Cells were treated with 0.5 μM or 1 μM vemurafenib ERK1/2 phosphorylated and unphosphorylated levels were monitored by immunoblotting and quantified by densitometric analysis; αTubulin was also examined to ensure equal loading of samples in each lane. f. mRNA levels of Cyclin D1 were determined by qRT-PCR analysis. g. Western blot analysis of cyclin d1. The Student's t-test was used to analyze the data. Error bars indicate mean ± SD; n = 3 experiments; *P < .05 indicates significant difference from DMSO treated cells. All the experiments were performed independently at least three times.

Western blotting analysis revealed that uPAR depletion decreased ERK1/2 and AKT phosphorylation compared to siCTRL-treated cells. However, the addition of vemurafenib to uPAR depleted culture, induced almost a complete disappearance of ERK phosphorylation, and a significant decrease of AKT phosphorylation (Fig. 3b). Notably, Vemurafenib treatment induced a substantial decrease of uPAR. Finally, we tested whether ectopic expression of uPAR was sufficient to lower vemurafenib sensitivity in A375 cells. We transduced EGFR/uPAR-low expressing A375 with Q2-uPAR expression vector and exposed these cells to treatment with increasing dose of Vemurafenib. Fig. 3c shows that A375 uPAR overexpressing cells became less sensitive to Vemurafenib as compared with the Mock control. Similar results were observed after forced uPAR expression in M6 cells (Fig. S2 c, d). The relative MAPK and PI3K/AKT signaling reported in Fig. 3d along with uPAR protein levels displays the less effectiveness of Vemurafenib on blocking ERK phosphorylation in presence of higher uPAR expression that concomitantly induces an increase on AKT phosphorylation. Taken together these results showed the uPAR might play an important role in the response to therapy therapy for the subgroup of melanoma patients with BRAF mutations.

Vemurafenib acquired resistance of M6 cells leads to the reactivation of the ERK pathway and confers fitness advantage in anchorage-independent growth.

To verify whether uPAR-EGFR targeted therapy is an effective strategy to overcome the acquired resistance to vemurafenib, we generated vemurafenib-resistant M6 (M6R) cells selected by continuous drug administration (Fig. 4a). First of all we analyzed the effects on cell cycle distribution in M6 parental cells (M6P) and in the generated vemurafenib resistant M6 after 24 h treatment with 1 μM or 2 μM

vemurafenib. As expected, the G1 cell cycle block and reduction of S-phase cells were pronounced and dose-dependent in the sensitive parental cells (Fig. 4b) while the vemurafenib-resistant M6 cells were insensitive to cell cycle arrest with >50% of the cell population in S phase at all the vemurafenib concentrations tested (Fig. 4c). We then evaluated the colony-forming ability of parental and vemurafenib-resistant cells after long-term treatment with increasing concentrations of the drug. As expected, we found that the vemurafenib-resistant cells required higher doses of vemurafenib up to 10uM for a significant growth inhibition (Fig. 4d). The reduced response to vemurafenib in the resistant cells went along with an elevated constitutive activity of the MAPK signaling pathway similar to that detected in parental M6 cultured in the absence of vemurafenib, whereas the level of pAKT and pMTOR were not consistently changed. As predictable, treatment of the wild type cells abrogated phosphorylation of ERK protein and led to an increased phosphorylation of the PI3K pathway proteins which is consistent with observations in literature [32,33]. Expression of unphosphorylated proteins was not altered by treatment (Fig. 4e). Since the anchorage-independent cell growth provides a useful tool for modeling tumor response to treatment in vitro and most closely mimics in vivo tumor growth, we measured the effect of vemurafenib on the potential growth in soft agar of parental and resistant cells. Treatment of M6 parental cells with a sole pulse of vemurafenib over 7 days substantially reduced colony size while marginally affected M6 resistant cells which were maintained for 4 days before the treatment in drug-free medium. In addition, resistant cells cultured in presence of the drug exibited a greater growth in soft agar than cells withdrawn from vemurafenib (Fig. 4f). Indeed, consistent with previous observation, resistant cells became addicted to the presence of the inhibitor
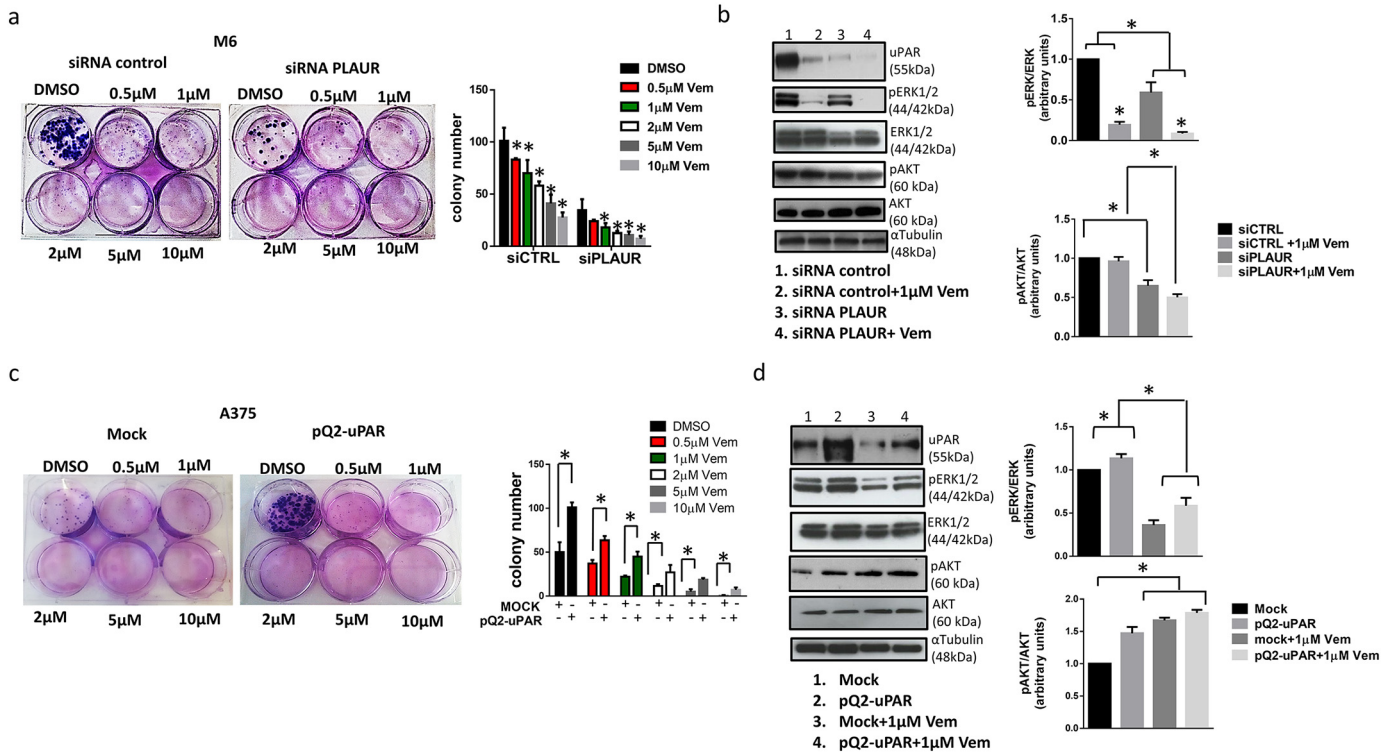
Fig. 3. uPAR overexpression prevents the sensitivity of melanoma cells to vemurafenib. a. M6 cells transfected with no targeting siRNA (siRNA Control) and a specific siRNA for uPAR. After 24 h the cells were seeded at the same density (800 cells/ml) and cultured in the presence of vemurafenib at indicated concentration for 10 days. The colonies were fixed, stained, photographed and counted. The Student's t-test was used to analyze the data. Error bars indicate mean ± SD; n = 3 experiments; *p < .05 indicates significant difference from DMSO treated cells b.M6 were transfected with PLAUR siRNA and negative control siRNA and incubated for 48 h in presence of 1 μM vemurafenib. Cells were harvested for immunoblotting with the indicated antibodies. αTubulin was included as a loading control. Densitometric analysis of the expression of the same proteins normalized to the internal control is reported on the right. Analysis of variance followed by Newman-Keuls post test was performed for comparing means of multiple groups. Error bars indicate mean ± SD; n = 3 experiments; *P < .05 indicate significant difference of vemurafenib treated cell from DMSO treated control, and of combo treatment (vemurafenib + siRNA PLAUR) versus either DMSO or vemurafenib treated cells. All the experiments were performed independently at least three times. c. A375 were transfected either with Mock or uPAR overexpressing plasmid pQ2-uPAR. After 24 h were seeded at the same density (800 cells/ml) and cultured in the presence of vemurafenib at indicated concentrations for 10 days. The colonies were fixed, stained, photographed and counted. Significance was assessed by Student's t-test. Error bars indicate mean ± SD; n = 3 experiments. *p < .05 indicates significant difference from DMSO treated cells. d. A375 Mock or uPAR transfected cells were harvested for Western blot analysis for the indicated antibodies. αTubulin was included as a loading control. Densitometric analysis of the expression of the same proteins normalized to the internal control is reported on the right. Significance was assessed by one-way ANOVA test followed by Newman-Keuls post test.Error bars indicate mean ± SD; Asterisks (*p < .05) indicate significant differences of vemurafenib treated cells, uPAR overexpressing cells or combo (vemurafenib + pQ2-uPAR) from Mock treated cells. All the experiments were performed independently at least three times.

resulting in greater growth in the presence of the inhibitor than without the drug.

3.4. Uncoupling uPAR and EGFR affects cellular proliferation, spheroid formation, 3D cell invasion

It has been shown by Liu and coworkers [34] that highly malignant tumor cells through overexpression of uPAR are able to exploit a tightly regulated EGFR pathway to obtain a proliferative advantage. On these basis, preventing the functional relationship between uPAR and EGFR emerges as a reasonable strategy to overcome acquired resistance. To assess whether uncoupling uPAR-EGFR interaction mediated by the alpha integrin chain could rescue the response to vemurafenib, resistant cells were treated with M25, a linear peptide known as integrin antagonist (Fig. 5a), in combination with vemurafenib. As shown in Fig. 5b, M25 and vemurafenib combination reduced the number of colonies of M6R to a significantly greater extent that M25 and vemurafenib alone. For comparison, we subjected the M6P to the same treatment and we observed a similar reduction of the colony number in presence of the combo.We then investigated the signaling pathway of the resistant and parental cells and their response to the combination treatment (Fig. 5c). As previously shown in Fig. 4 E, the enhanced ERK activity was maintained in M6R cells even following BRAF inhibition, while it was strongly reduced in the parental cell line. Compared to single agents alone the combination treatment synergistically reduces pAKT and

pERK levels in M6R (Fig. 5c), while in the parental cell line we observed a synergistic effect of M25 + Vem on ERK phosphorylation alongside a significant reduction of AKT phosphorylation either after M25 treatment or M25 + Vem. Moreover either M25 or the combo (M25 + vemurafenib) abrogated mTOR phosphorylation in both cell lines. Since the dominant mechanism of resistance to vemurafenib in M6R resulted in MEK/ERK signaling reactivation, we evaluated whether these cells retained the sensitivity to MEK1/2 or ERK1/2 inhibitors. Consistent with previous findings [35,36], we observed a significant reduction of ERK1/2 phosphorylation after 24 h treatment with 1 μM of CI-1040 as MEK1/2 inhibitor while a visible decrease was found in presence of 1 μM SCH772984 as ERK1/2 inhibitor. We also detected a slight increase of AKT phosphorylation after either MEK1/2 or ERK1/2 inhibition. Nevertheless the combination of either inhibitors with M25 resulted in a more pronounced decrease of ERK phosphorylation and EGFR protein levels along with a synergistic reduction of pAKT (Fig. S3a). As previously shown (Figs. 4E and 5C) no changes were detected in presence of vemurafenib (Fig. S3a). Morphological modification were observed either with single MEK1/2 or ERK1/2 inhibitors alone or in combination with M25 (fig. S3b).Since the effectiveness of M25 was more accurately significant in combination with vemurafenib we then evaluated the potential effect of this combination treatment on an important feature of cancer cells, such as cell invasion (Fig. 5d and Fig. S4). We performed cancer cell invasion in a three-dimensional matrix, which is more representative of how these cells will actually behave in vivo. In our
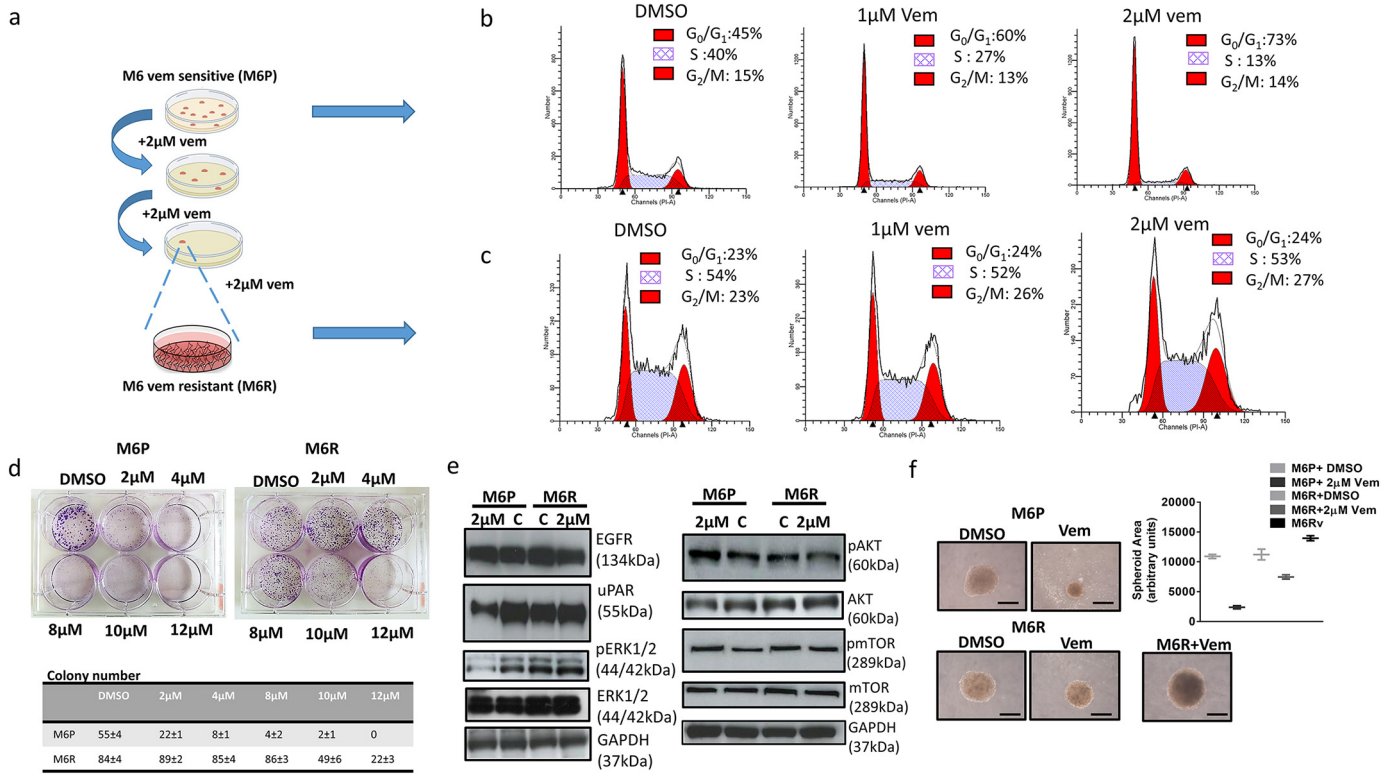
Fig. 4. Analysis of the biological and molecular features of naïve cells and its BRAF-resistant counterpart a. Schematic representation of the induced vemurafenib resistance protocol in M6 cells. b. M6 vem sensitive (M6P) cells and c, M6 vem resistant cells (M6R), were treated for 24 h with DMSO or the indicated doses of vemurafenib, stained with propidium iodide, and analyzed for cell cycle progression by flow cytometry. Representative images from one of three independent experiments are shown. The percentage of cells in the different phases of the cell cycle was calculated by the ModFit program and depicted in each panel. d. M6P and M6R cells (800 cells/ml) were exposed to graded concentrations of vemurafenib for ten days. Colonies were stained with May Grunwald and the counts reported in the related table. Representative data of three independent experiments is shown (mean ± SD). e. Immunoblot analysis for AKT, ERK1/2 and mTOR activity in M6R and M6P untreated or treated for 24 h with 2 μM vemurafenib. GAPDH was used as loading control. f. Images of M6P and M6R spheroids on agar coated plates following treatment with DMSO or μM vemurafenib. Spheroid area is reported on the right. Scale bar = 200 μm.

experiment we used matrigel as ECM material and we quantified cell invasion as a function of the total area invaded by cells leaving the spheroid. As shown in Fig. 5d, M6R cells acquire a more invasive phenotype compared to parental cells. However, the combination strongly impaired invasion compared to the single agents alone. (Fig. 5d). Spheroids are supposed to better reflect the in vivo conditions with respect to drug efficacy. Cell-cell interaction governs the growth, the ability to maintain the spheroid shape, and affects the drug permeability. In particular, we observed that the combination treatment dramatically reduced the spheroid core area compared to the single agents alone. Moreover, M25 and M25 plus vemurafenib treatment affected spheroid shape that indeed started to dismantle and cells became separated from each other, leading likely to cell death, whereas vemurafenib-treated spheroid showed a solid round core (Fig. 5e). Immunoprecipitation experiments demonstrated that the effectiveness of M25 at molecular and biological levels on M6R was due to the ability of this peptide to uncouple uPAR from α5β1 and consequently from EGFR (Fig. 5f). Confocal immuno-fluorescence analysis of integrin β1/uPAR (Fig. 5g) and uPAR/EGFR (Fig. S5) confirmed the abrogation of the interaction in presence of the M25 peptide in M6R as previously observed in M6 wt [37]. All together these results showed that uPAR actively participate to vemurafenib unresponsiveness to BRAF-I in resistant cells and thus, uncoupling EGFR/uPAR interaction represents a promising tool to overcome the acquired resistance.

3.5. Paired high levels of uPAR and EGFR expression correlate in tissue samples from relapsed patients

Formalin-fixed paraffin-embedded (FFPE) specimens represent a reliable clinical source of molecular signatures with great potential of predictive features for patient therapy stratification. To evaluate the possible clinical implications of our in vitro findings, we examined uPAR and EGFR gene expression in tumor biopsies from six patients with metastatic melanoma (Fig. 6 A) before the BRAF inhibitor Vemurafenib treatment. The tumors of all six patients were BRAF^{V600E+} and initially responded to treatment with Vemurafenib but five of them (patients #2, 3, 4, 5 and 6) relapsed after 3–15 months, suggesting that they developed resistance to the BRAF inhibitor and died shortly afterwards. As we were particularly interested in our signature's drug response performance, we chose to adopt the progression as a measure of response/non-response comparing the uPAR and EGFR levels in relapsed patients with those of patient #1 who achieved the complete response and is still alive (Fig. 6B). As reported in fig. 6C we found detectable uPAR levels in 4 relapsed patients: two of them exhibited very high levels (mRNA relative values ranged from 15 to 53), two of them moderate levels (1.3 to 2.7). Nevertheless, EGFR mRNA levels could be quantified in three out of 5 five relapsed patients (relative values fluctuated from 8 to 30). Interestingly, patient #5 with the highest uPAR levels displayed a concomitant strongest increase of EGFR expression. Although the number of specimens examined was small, due to limited number of patient subjected to vemurafenib monotherapy, our findings suggest that uPAR expression or EGFR could represent a predictive value towards the determination of patient responsiveness to BRAF inhibitor-based therapies and provide insight into future therapies for the treatment of patients who become refractory to these drugs.

4. Discussion

Acquired resistance to the small molecule BRAF inhibitor, Vemurafenib (PLX4032), represents the major drawback limiting
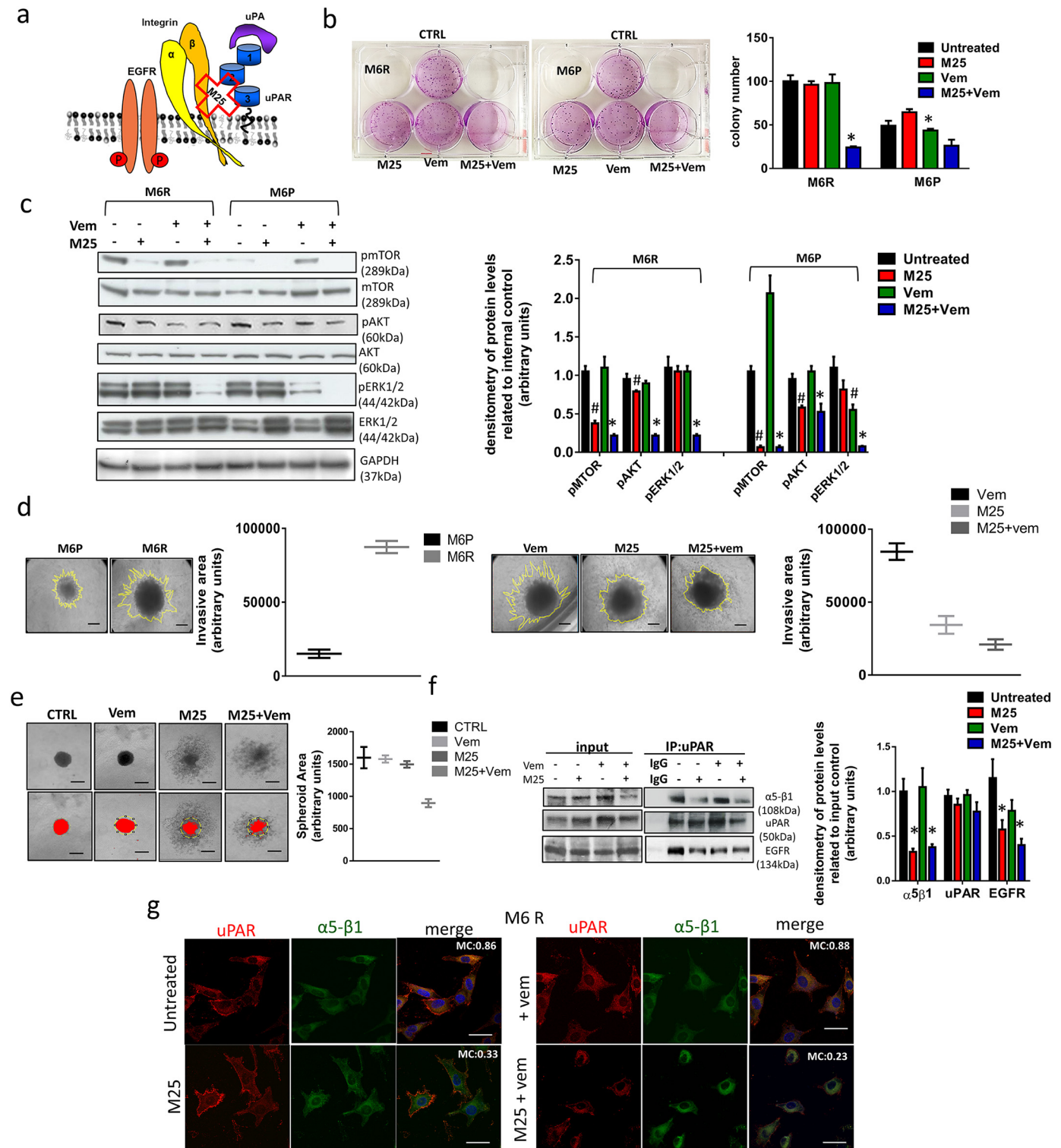
successful, long term clinical benefit for patients with malignant melanomas that harbor the V600E BRAF mutation [38–41]. Consequently, much effort is being focused at identifying the cellular and molecular mechanisms involved in resistance to BRAF-targeted therapy in these tumors. The present study is a contribution to these efforts, the results provide important novel insight into the complexity of the vemurafenib resistance phenotype in melanoma and advance the basis upon which such resistance may be overcome clinically. To mimic the clinical situation in which resistance to vemurafenib frequently occurs after the initial response to the cure, we induced in vitro vemurafenib resistance in a

BRAF-I sensitive human melanoma cell line M6, harboring the V600E BRAF mutation, by continuous exposure of the cells to vemurafenib. We considered as an acquired resistance when melanoma cells regained their original level of proliferation (Fig. 4C and F) and then, we i) evaluated the biological behavior of naïve cells and their vemurafenib-resistant counterpart; ii) investigated the molecular signatures, in particular those related to MAPK and PI3K signaling, associated with the acquisition of vemurafenib resistance. Our study not only establishes a mechanism of resistance to BRAF inhibition but also proposes a strategy to overcome it.

In this paper we provide a strong evidence that the well known and characterized uPA receptor (uPAR) acts not only as a promoter of proliferation, invasiveness and angiogenesis in melanoma and other cancer cell lines [42–45] but also as a factor contributing to the development of drug resistance. Indeed, we found a remarkable direct association between uPAR and EGFR co-expression levels and vemurafenib responsiveness inV600E BRAF mutated melanoma cells. Noteworthy the distinctive and simultaneous expression of both uPAR and EGFR protein levels in three out of seven cell lines was associated with the higher phosphorylated levels of ERK1/2.

In the first instance we show that lower expression levels of uPAR and EGFR, displayed by A375 cells, are associated with higher vemurafenib sensitivity as confirmed by clonogenic assay and short term cell viability. The link with drug responsiveness was further validated in a set of clonogenic assays, which proved how uPAR enforced expression in A375 (Fig. 3d) and M6 (Fig. S2c) cells was able to revert drug sensitivity to the BRAF inhibitor suggesting that uPAR overexpression renders melanomas less susceptible to the targeted inhibitor. Quite the opposite, we demonstrated that uPAR knockdown in A375 cells (Fig. S2b) and also in M6 (Fig. 3b), which exhibited higher uPAR and EGFR levels compared to A375 cells, inhibited cell proliferation in combination with vemurafenib to a greater extent than either treatment alone. The direct involvement of uPAR was confirmed by the fact that enforced overexpression did not affect EGFR levels and even more by the fact that its gene silencing paradoxically induces an EGFR slight increase. Taken together, these data indicate that uPAR plays a direct role in vemurafenib responsiveness and inhibiting uPAR represents a novel strategy to enhance melanoma sensitivity to BRAF-I.

At the molecular level we proved that uPAR was able to simultaneously affect the two pathways required for BRAF mutated melanomas to proliferate (BRAF/MAPK and PI3K pathways), since inhibition of its expression by uPAR-specific siRNA causes a reduction of ERK and AKT activation and restores sensitivity to BRAF-I. This explains why uPAR depletion is effective as single agent in the colony formation capacity in the absence of vemurafenib, even though there is clear synergism between uPAR knockdown and BRAF inhibitor. Moreover we found that in sensitive cells Vemurafenib itself strongly decreased uPAR protein levels (Fig. 4e) which reverts to control levels after Vemurafenib acquired resistance and correlates with p- ERK1/2 levels, suggesting reactivation of the BRAF signaling pathway (Figs. 4e and 5c).
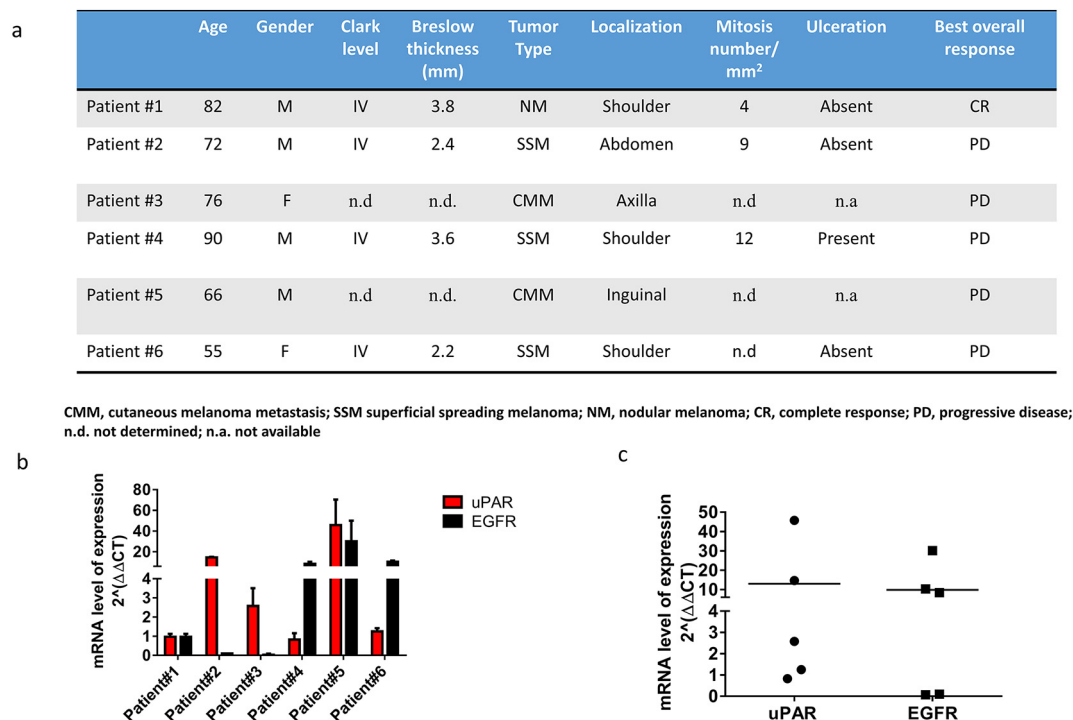
As a matter of fact, uPAR is a glycosylphosphatidylinositol-anchored membrane protein which associates with integrins and RTKs such as EGFR to form a potent signaling complex [31,37,45].uPAR is overexpressed in many human malignancies including melanomas [46–49] and is associated with a worse prognosis especially among breast cancer and esophageal carcinomas. Our previous findings, along with the results obtained in other studies, showed that uPAR is an indispensable molecular mediator, in concert with integrin, of tumor growth, cell invasion and angiogenesis [31,37,45].Since the resistance to treatment with single inhibitors of the MAPK pathway commonly emerges, experimental combinatorial therapies have been launched [50,51]. But early clinical data on BRAF mutant melanoma patients treated with a combinatorial approach of BRAF and MEK inhibitors (dabrafenib + trametinib) indicates that, unfortunately, even in that setting eventually most patients relapse.

Thus, addition of an alternative or third compound prolonging clinical response is highly needed. We set out to demonstrate that uPAR and EGFR interaction may be successfully leveraged as a novel pharmacologic target in M6R. There are a number of previous studies that have reported the role of the uPAR-integrin-EGFR relationship, leading to define the so-called "urokinase receptor interactome" [21]. The natural follow-up of such studies has resulted into attempts to target the uPAR-integrin-EGFR axis to reduce the "classical" uPAR and EGFR-dependent cancer signatures (invasion and proliferation) [20,52–61]. Following the beginning of targeted and personalized cancer therapy, characterized by the use of new cancer-specific molecules (such as vemurafenib and anti-EGFR antibodies), some studies have addressed the problem of overcoming pharmacological resistance to such new therapeutics, upon identification of a role of RTKs in the onset of resistance [62,63]. In view of its integrin-mediated interaction with some RTKs (and in particular with EGFR), malignancy-linked uPAR overexpression has become a natural candidate in resistance-addressed studies [64,65]. In particular, Tyrosine kinase inhibitor Gefitinib (IRESSA, ZD 1839), commonly used in mono-therapy for the treatment of non small cell lung cancer (NSCLC) harboring an activating mutation of EGFR-tyrosine kinase, significantly reduces EGFR and ERK activation. Combining uPAR down-regulation with IRESSA-dependent EGFR inhibition, showed a synergistic anti-tumor effect in malignant cells of head and neck cancers and in a series of immortalized cancer cell lines [66,67].

In this study we proved the efficacy in vitro of M25, a linear peptide known as integrin antagonist in combination with vemurafenib in overcoming BRAF-I acquired resistance. We found that preventing by M25 the integrin-dependent interaction between uPAR and EGFR restores the vemurafenib sensitivity in acquired BRAF inhibitor resistant cells by affecting the BRAF/MAPK and PI3K pathways: blocking integrin-mediated uPAR-TKRs interaction, while inhibiting the PI3K pathaway, reactivates the BRAF/MAPK pathway, hence refueling the vemurafenib-sensitive substrates and hindering the PI3K escape signaling pathway. We believe that its potency in the inhibition of 2D and 3D cell proliferation as well as in cell invasion has to be attributed to its interference with these two complementary pathways. These results provide a rationale for clinically exploring the inhibition of EGFR/uPAR interaction to overcome resistance in uPAR-high, BRAF-mutant

Fig. 5. Effect of the combination of Vemurafenib and M25 on the growth, invasion, PI3K and MAPK signaling pathways of M6R. a. Schematic representation of integrin, EGFR and uPAR interaction. b. Clonogenic assay of M6R and M6P treated with vemurafenib, M25 or the combo (vemurafenib + M25) for 10 days. Colonies were stained, and then counted. One-way ANOVA test followed by Newman-Keuls post test was used to determine the significance of combination treatments versus control and single treatments. Error bars indicate mean ± SD; n = 3 experiments; Asterisks indicate significant differences (P < .05.) of the combo versus untreated, vemurafenib or M25 treated cells.c.M6R and M6P treated for 24 h with M25 or vemurafenib, either administered alone or in combination were harvested for immunoblotting with the indicated antibodies. GAPDH was included as a loading control. Relative protein phosphorylation levels of AKT, ERK1/2 and mTOR were quantified by densitometry and reported as values normalized to the GAPDH. Significance was assessed by one-way ANOVA test followed by Newman-Keuls post test.Error bars indicate mean ± SD; n = 3 experiments; Asterisks indicate significant differences (P < .05.) of the combo treatment from DMSO-treated, while number signs indicate significant differences (P < .05) of either M25 or Vemurafenib alone from DMSO-treated cells. d. Representative images and invasive area quantification of M6P and M6R spheroids embedded into the matrigel substrate in presence of either vemurafenib or M25 administered alone or in combination. Cell sprouting and invasion cells are depicted in yellow. Scale bar = 200 μm.Measures of invasive areas (invasive area = total area-spheroid area) are reported in graphs on the right panel. On the left, comparative pictures of M6P and M6R invasive spheroids with the relative invasive area quantification. e. Representative images of spheroids on agar-coated plates of M6R in presence of either vemurafenib or M25 administered alone or in combination. M6R cells were pre-incubated with Vemurafenib, M25 or the combo for 24 h. Scale bar = 1 mm. f. Immunoprecipitation of α5β1-integrin. Input: Western blotting of aliquots (30 μg of proteins) of cell lysates before immunoprecipitation, used as a reference loading control. IP uPAR: immunoprecipitate (500 μg of proteins) obtained with anti-uPAR R5 antibody; alpha5-beta1 lane: immunoblotting with anti-α5β1 antibody; uPAR lane: immunoblotting with anti-uPAR antibody; EGFR lane: immunoblotting with EGFR antibody: IgG a lysate that was incubated with non-specific IgG instead of the antibody and used as negative control. Densitometric quantification of the immunoblots normalized to the relative input is reported on the right. Significance was assessed by one-way ANOVA test followed by Newman-Keuls post test.Error bars indicate mean ± SD; Asterisks (p < .05) indicate significant differences of either M25 or the combo treatment from DMSO-treated. Experiments have been performed three times in triplicate with similar results. g. Representative images of confocal microscopy of companion M6R treated cultures stained with specific anti-uPAR (red), α5β1 (green) and DAPI (blue). Experiments have been performed three times in triplicate with analogous results. The co-localization score is quantified by image J andreported within each picture as Manders' coefficient (MC). The shown pictures are representative of 20 different pictures for each experimental condition. Scale bar = 20 μm.

a

	Age	Gender	Clark level	Breslow thickness (mm)	Tumor Type	Localization	Mitosis number/ mm²	Ulceration	Best overall response
Patient #1	82	M	IV	3.8	NM	Shoulder	4	Absent	CR
Patient #2	72	M	IV	2.4	SSM	Abdomen	9	Absent	PD
Patient #3	76	F	n.d	n.d.	CMM	Axilla	n.d	n.a	PD
Patient #4	90	M	IV	3.6	SSM	Shoulder	12	Present	PD
Patient #5	66	M	n.d	n.d.	CMM	Inguinal	n.d	n.a	PD
Patient #6	55	F	IV	2.2	SSM	Shoulder	n.d	Absent	PD

CMM, cutaneous melanoma metastasis; SSM superficial spreading melanoma; NM, nodular melanoma; CR, complete response; PD, progressive disease; n.d. not determined; n.a. not available

b

c

Fig. 6. uPAR and EGFR expression levels on tumor biopsies of metastatic melanoma patients before vemurafenib treatment: predictive values to BRAF-I responsiveness? A, Biological and clinical data of the six metastatic melanoma patients treated with vemurafenib as monotherapy. B, Level of uPAR and EGFR expression on isolated micrometastatic cells in 6 patients. Relative EGFR and uPAR expression levels compared to mRNA 18S and GAPDH on formalin-fixed paraffin embedded (FFPE) melanoma tissue sections from BRAF(V600E) mutant melanoma patients. C, Scatter plots depicted direct correlation between uPAR and EGFR in relapsed patients Experiments have been performed three times in triplicate with similar results.

melanomas. Noteworthy, it has been reported that pharmacological inhibition of BRAFV600E suppresses the recruitment of tumor-promoting cell subsets such as Myeloid Derived Suppressor Cells and regulatory T cells in tumor microenvironments and, on the contrary, sensitizes the immune system to target tumors by inducing an upregulation of the expression of melanoma/melanocyte differentiation antigens MART-1, gp100 and tyrosinase [68,57]. Thus, restoring vemurafenib responsiveness in resistant cells by targeting uPAR/EGFR interaction may pave the way to enhance antitumor immunity and, in combination with immunotherapy, may lead to more potent, durable and better individualized treatment in patients with advanced melanoma.

With the aim of pursuing our initial findings on the role of uPAR in mediating resistance to ERK inhibition, we tried to corroborate these results in the context of relapsing melanoma patients. From a cohort of 6 patients, we found uPAR to be upregulated in four patients relapsed with resistant melanoma. In comparison, EGFR gain was found in three patients. Interestingly one patient in this cohort displayed simultaneous expression of both uPAR and EGFR. Since almost all the relapsed patients displayed significant levels of uPAR these data suggested that uPAR may be a useful biomarker to identify patients with BRAF-mutant melanoma who will or will not respond to BRAF-I.

In conclusion, we showed that high levels of uPAR lower the sensitivity to vemurafenib in BRAF mutant cells while uPAR loss of function increases their susceptibility to vemurafenib and restores responsiveness in BRAF-I-acquired resistant cells. Understanding the mechanisms of interaction between uPAR and different tyrosine kinase receptors (RTK) offers the potential to reveal new opportunities for overcoming drug resistance and to design drug combinations that will lead to more potent, durable individualized treatment.

Declaration of interests

The authors declare no potential conflicts of interest.

Authors' contributions

A.L. conceived, designed the study. F.M. and A.C. performed clonogenic assays and developed the methodology. J.R., S.P., S.S., A.B., E.A. performed transfection experiment and acquired data. F.M., A.L. and A.B., analyzed and interpreted the data. G.F., M.D.R., L.D. and A.L. wrote, reviewed and revised the manuscript. M.D.R. obtained funding and revised the manuscript. N.P. provided tissue specimens, designed the clinical experiments and analyzed the data.

Appendix A. Supplementary data

Supplementary data to this article can be found online at https://doi.org/10.1016/j.ebiom.2018.12.024.

References

[1] Alexandrov LB, Nik-Zainal S, Wedge DC, Aparicio SA, Behjati S, Biankin AV, et al. Signatures of mutational processes in human cancer. Nature 2013;500:249–56.
[2] Comis RL. DTIC (NSC-45388) in malignant melanoma: a perspective. Cancer Treat Rep 1976;60:165–76.

[3] Tsao H, Atkins MB, Sober AJ. Management of cutaneous melanoma. N Engl J Med 2004;351:998–1012.

[4] Atkins MB, Lotze MT, Dutcher JP, Fisher RI, Weiss G, Margolin K, et al. High-dose recombinant interleukin 2 therapy for patients with metastatic melanoma: analysis of 270 patients treated between 1985 and 1993. J Clin Oncol 1999;17:2105–16.

[5] Rosenberg SA, Yang JC, Sherry RM, Kammula US, Hughes MS, Phan GQ, et al. Durable complete responses in heavily pretreated patients with metastatic melanoma using T-cell transfer immunotherapy. Clin Cancer Res 2011;17:4550–7.

[6] Padua RA, Barrass N, Currie GA. A novel transforming gene in a human malignant melanoma cell line. Nature 1984;311:671–3.

[7] Sekulic A, Haluska PJ, Miller AJ, Genebriera De Lamo J, Ejadi S, Pulido JS, et al. Malignant melanoma in the 21st century: the emerging molecular landscape. Mayo Clinic Proceedings. Mayo Clinic; 2008. p. 825–46.

[8] Brose MS, Volpe P, Feldman M, Kumar M, Rishi I, Gerrero R, et al. BRAF and RAS mutations in human lung cancer and melanoma. Cancer Res 2002;62:6997–7000.

[9] Davies H, Bignell GR, Cox C, Stephens P, Edkins S, Clegg S, et al. Mutations of the BRAF gene in human cancer. Nature 2002;417:949–54.

[10] Sosman JA, Kim KB, Schuchter L, Gonzalez R, Pavlick AC, Weber JS, et al. Survival in BRAF V600-mutant advanced melanoma treated with vemurafenib. N Engl J Med 2012;366:707–14.

[11] Trunzer K, Pavlick AC, Schuchter L, Gonzalez R, McArthur GA, Hutson TE, et al. Pharmacodynamic effects and mechanisms of resistance to vemurafenib in patients with metastatic melanoma. J Clin Oncol 2013;31:1767–74.

[12] Tentori L, Lacal PM, Graziani G. Challenging resistance mechanisms to therapies for metastatic melanoma. Trends Pharmacol Sci 2013;34:656–66.

[13] Sabbatino F, Wang Y, Wang X, Flaherty KT, Yu L, Pepin D, et al. PDGFRα upregulation mediated by sonic hedgehog pathway activation leads to BRAF inhibitor resistance in melanoma cells with BRAF mutation. Oncotarget 2014;5:1926–41.

[14] Ruzzolini J, Peppicelli S, Andreucci E, Bianchini F, Margheri F, Laurenzana A, et al. Everolimus selectively targets vemurafenib resistant BRAFV600E melanoma cells adapted to low pH. Cancer Lett 2017;408:43–54.

[15] Poulikakos PI, Persaud Y, Janakiraman M, Kong X, Ng C, Moriceau G, et al. RAF inhibitor resistance is mediated by dimerization of aberrantly spliced BRAF(V600E). Nature 2011;480:387–90.

[16] Blasi F, Carmeliet P. uPAR: a versatile signalling orchestrator. Nat Rev Mol Cell Biol 2002;3:932–43.

[17] Dass K, Ahmad A, Azmi AS, Sarkar SH, Sarkar FH. Evolving role of uPA/uPAR system in human cancers. Cancer Treat Rev 2008;34:122–36.

[18] Busso N, Masur SK, Lazega D, Waxman S, Ossowski L. Induction of cell migration by pro-urokinase binding to its receptor: possible mechanism for signal transduction in human epithelial cells. J Cell Biol 1994;126:259–70.

[19] Poettler M, Unseld M, Mihaly-Bison J, Uhrin P, Koban F, Binder BR, et al. The urokinase receptor (CD87) represents a central mediator of growth factor-induced endothelial cell migration. Thromb Haemost 2012;108:357–66.

[20] Hu J, Muller KA, Furnari FB, Cavenee WK, Vandenberg SR, Gonias SL. Neutralizing the EGF receptor in glioblastoma cells stimulates cell migration by activating uPAR-initiated cell signaling. Oncogene 2015;34:4078–88.

[21] Eden G, Archinti M, Furlan F, Murphy R, Degryse B. The urokinase receptor interactome. Curr Pharm Des 2011;17:1874–89.

[22] Ossowski L, Aguirre-Ghiso JA. Urokinase receptor and integrin partnership: coordination of signalling for cell adhesion, migration and growth. Curr Opin Cell Biol 2000;12:613–20.

[23] Tarui T, Mazar AP, Cines DB, Takada Y. Urokinase-type plasminogen activator receptor CD87 is a ligand for integrins and mediates cell-cell interaction. J Biol Chem 2001;276:3983–90.

[24] Hu J, Jo M, Cavenee WK, Furnari F, Vandenberg SR, Gonias SL. Crosstalk between the urokinase-type plasminogen activator receptor and EGF receptor variant III supports survival and growth of glioblastoma cells. Proc Natl Acad Sci U S A 2011;108:15984–9.

[25] Kiyan J, Kiyan R, Haller H, Inna Dumler I. Urokinase-induced signaling in human vascular smooth muscle cells is mediated by PDGFR-β. EMBO J 2005;24:1787–97.

[26] Runge DM, Runge D, Dorko K, Pisarov LA, Leckel K, Kostrubsky VE, et al. Epidermal growth factor- and hepatocyte growth factor-receptor activity in serum-free cultures of human hepatocytes. J Hepatol 1999;30:265–74.

[27] Perna D, Karreth FA, Rust AG, Perez-Mancera PA, Rashid M, Iorio F, et al. BRAF inhibitor resistance mediated by the AKT pathway in an oncogenic BRAF mouse melanoma model. Proc Natl Acad Sci U S A 2015;112:E536–45.

[28] Eisenhauer EA, Therasse P, Bogaertsc J, Schwartz LH, Sargent D, Ford R, et al. New response evaluation criteria in solid tumours: Revised RECIST guideline (version 1.1). Eur J Cancer 2009;45:228–47.

[29] Bonin S, Stanta G. Nucleic acid extraction methods from fixed and paraffin-embedded tissues in cancer diagnostics. Expert Rev Mol Diagn 2013;13:271–82.

[30] Sun C, Wang L, Huang S, Heynen GJ, Prahallad A, Robert C, et al. Reversible and adaptive resistance to BRAF(V600E) inhibition in melanoma. Nature 2014;508:118–22.

[31] Laurenzana A, Chillà A, Luciani C, Peppicelli S, Biagioni A, Bianchini F, et al. uPA/uPAR system activation drives glycolytic phenotype in melanoma cells. Int J Cancer 2017;141:1190–200.

[32] Steelman LS, Chappell WH, Abrams SL, Kempf RC, Long J, Laidler P, et al. Roles of the Raf/MEK/ERK and PI3K/PTEN/Akt/mTOR pathways in controlling growth and sensitivity to therapy-implications for cancer and aging. Aging (Albany NY) 2011;3:192–222.

[33] Turke AB, Song Y, Costa C, Cook R, Arteaga CL, Asara JM, et al. MEK inhibition leads to PI3K/AKT activation by relieving a negative feedback on ERBB receptors. Cancer Res 2012;72:3228–37.

[34] Liu D, Aguirre Ghiso J, Estrada Y, Ossowski L. EGFR is a transducer of the urokinase receptor initiated signal that is required for in vivo growth of a human carcinoma. Cancer Cell 2002;1:445–57.

[35] Carlino MS, Todd JR, Gowrishankar K, Mijatov B, Pupo GM, Fung C, et al. Differential activity of MEK and ERK inhibitors in BRAF inhibitor resistant melanoma. Mol Oncol 2014;8:544–54.

[36] Wong DJL, Robert L, Atefi MS, Lassen A, Avarappatt G, Cerniglia M, et al. Antitumor activity of the ERK inhibitor SCH722984 against BRAF mutant, NRAS mutant and wild-type melanoma. Mol Cancer 2014;13:194–208.

[37] Margheri F, Luciani C, Taddei ML, Giannoni E, Laurenzana A, Biagioni A, et al. The receptor for urokinase-plasminogen activator (uPAR) controls plasticity of cancer cell movement in mesenchymal and amoeboid migration style. Oncotarget 2014;5:1538–53.

[38] Bollag G, Hirth P, Tsai J, Zhang J, Ibrahim PN, Cho H, et al. Clinical efficacy of a RAF inhibitor needs broad target blockade in BRAF-mutant melanoma. Nature 2010;467:596–9.

[39] Poulikakos PI, Zhang C, Bollag G, Shokat KM, Rosen N. RAF inhibitors transactivate RAF dimers and ERK signalling in cells with wild-type BRAF. Nature 2010;464:427–30.

[40] Su F, Viros A, Milagre C, Trunzer K, Bollag G, Spleiss O, et al. RAS mutations in cutaneous squamous-cell carcinomas in patients treated with BRAF inhibitors. N Engl J Med 2012;366:207–15.

[41] Wagle N, Emery C, Berger MF, Davis MJ, Sawyer A, Pochanard P, et al. Dissecting therapeutic resistance to RAF inhibition in melanoma by tumor genomic profiling. J Clin Oncol 2011;29:3085–96.

[42] Ciavarella S, Laurenzana A, De Summa S, Pilato B, Chillà A, Lacalamita R, et al. uPAR expression in cancer associated fibroblast: new acquisitions in multiple myeloma progression. BMC Cancer 2017;17:215.

[43] Laurenzana A, Biagioni A, Bianchini F, Peppicelli S, Chillà A, Margheri F, et al. Inhibition of uPAR-TGFβ crosstalk blocks MSC-dependent EMT in melanoma cells. J Mol Med (Berl) 2015;93:783–94.

[44] D'Alessio S, Margheri F, Pucci M, Del Rosso A, Monia BP, Bologna M, et al. Antisense oligodeoxynucleotides for urokinase-plasminogen activator receptor have anti-invasive and anti-proliferative effects in vitro and inhibit spontaneous metastases of human melanoma in mice. Int J Cancer 2004;110:125–33.

[45] Chilla A, Margheri F, Biagioni A, Del Rosso M, Fibbi G, Laurenzana A. Mature and progenitor endothelial cells perform angiogenesis also under protease inhibition: the amoeboid angiogenesis. J Exp Clin Cancer Res 2018;37:74–88.

[46] de Witte JH, Foekens JA, Brunner N, Heuvel JJ, van Tienoven T, Look MP, et al. Prognostic impact of urokinase-type plasminogen activator receptor (uPAR) in cytosols and pellet extracts derived from primary breast tumours. Br J Cancer 2001;85:85–92.

[47] Heiss MM, Allgayer H, Gruetzner KU, Funke I, Babic R, Jauch KW, et al. Individual development and uPA-receptor expression of disseminated tumour cells in bone marrow: a reference to early systemic disease in solid cancer. Nat Med 1995;1:1035–9.

[48] Heiss MM, Simon EH, Beyer BC, Gruetzner KU, Tarabichi A, Babic R, et al. Minimal residual disease in gastric cancer: evidence of an independent prognostic relevance of urokinase receptor expression by disseminated tumor cells in the bone marrow. J Clin Oncol 2002;20:2005–16.

[49] Allgayer H, Heiss MM, Riesenberg R, Grützner KU, Tarabichi A, Babic R, et al. Urokinase plasminogen activator receptor (uPA-R): one potential characteristic of metastatic phenotypes in minimal residual tumor disease. Cancer Res 1997;57:1394.

[50] Kim KB, Kefford R, Pavlick AC, Infante JR, Ribas A, Sosman JA, et al. Phase II study of the MEK1/MEK2 inhibitor Trametinib in patients with metastatic BRAF-mutant cutaneous melanoma previously treated with or without a BRAF inhibitor. J Clin Oncol 2013;31:482–9.

[51] Acciardo S, Mignion L, Joudiou N, Bouzin C, Baurain JF, Gallez B, et al. Imaging markers of response to combined BRAF and MEK inhibition in BRAF mutated vemurafenib-sensitive and resistant melanomas. Oncotarget 2018;9:16832–46.

[52] Jo M, Thomas KS, Marozkina N, Amin TJ, Silva CM, Parsons SJ, et al. Dynamic assembly of the urokinase-type plasminogen activator signaling receptor complex determines the mitogenic activity of urokinase-type plasminogen activator. J Biol Chem 2005;280:17449–57.

[53] Mazzieri R, D'Alessio S, Kamgang Kenmoe R, Ossowski L, Blasi F. An uncleavable uPAR mutant allows dissection of signaling pathways in uPA-dependent cell migration. Mol Biol Cell 2006;17:367–78.

[54] Lee EJ, Whang JH, Jeon NK, Kim J. The epidermal growth factor receptor tyrosine kinase inhibitor ZD1839 (Iressa) suppresses proliferation and invasion of human oral squamous carcinoma cells via p53 independent and MMP, uPAR dependent mechanism. Ann N Y Acad Sci 2007;1095:113–28.

[55] Jo M, Thomas KS, Takimoto S, Gaultier A, Hsieh EH, Lester RD, et al. Urokinase receptor primes cells to proliferate in response to epidermal growth factor. Oncogene 2007;26:2585–94.

[56] D'Alessio S, Gerasi L, Blasi F. uPAR-deficient mouse keratinocytes fail to produce EGFR-dependent laminin-5, affecting migration in vivo and in vitro. J Cell Sci 2008;121:3922–32.

[57] Larusch GA, Merkulova A, Mahdi F, Shariat-Madar Z, Sitrin RG, Cines DB, et al. Domain 2 of uPAR regulates single-chain urokinase-mediated angiogenesis through β1-integrin and VEGFR2. Am J Physiol Heart Circ Physiol 2013;305:H305–20.

[58] Hu J, Jo M, Cavenee W, Furnari F, Vandenberg SR, Gonias SL. Crosstalk between the urokinase-type plasminogen activator receptor and EGF receptor variant III supports survival and growth of glioblastoma cells. Proc Natl Acad Sci U S A 2011;108:15984–9.

[59] Eden G, Archinti M, Arnaudova R, Andreotti G, Motta A, Furlan F, et al. D2A sequence of the urokinase receptor induces cell growth through αvβ3 integrin and EGFR. Cell Mol Life Sci 2018;75:1889–907.

[60] Furlan F, Eden G, Archinti M, Arnaudova R, Andreotti G, Citro V, et al. D2A-Ala peptide derived from the urokinase receptor exerts anti-tumoral effects in vitro and in vivo. Peptides 2018;101:17–24.

[61] Prahallad A, Sun C, Huang S, Di Nicolantonio F, Salazar R, Zecchin D, et al. Unresponsiv-eness of colon cancer to BRAF(V600E) inhibition through feedback activation of EGFR. Nature 2012;483:100–3.

[62] Girotti MR, Marais R. Deja Vu: EGF receptors drive resistance to BRAF inhibitors. Cancer Discov 2013;3:487–90.

[63] Gonias SL, Hu J. Urokinase receptor and resistance to targeted anticancer agents. Front Pharmacol 2015;6:154–60.

[64] Wykosky J, Hu J, Gomez GG, Taylor T, Villa GR, Pizzo D, et al. A urokinase receptor-Bim signaling axis emerges during EGFR inhibitor resistance in mutant EGFR glioblastoma. Cancer Res 2015;75:394–404.

[65] Abu-Ali S, Fotovati A, Shirasuna K, Furet P, Schnell C, Fritsch C, et al. Tyrosine-kinase inhibition results in EGFR clustering at focal adhesions and consequent exocytosis in uPAR down-regulated cells of Head and Neck cancers. Mol Cancer 2008;7:47–60.

[66] Di Mauro C, Pesapana A, Formisano L, Rosa R, D'Amato V, Ciciola P, et al. Urokinase-type plasminogen activator receptor (uPAR) expression enhances invasion and metastasis in RAS mutated tumors. Sci Rep 2017;7:9388–400.

[67] Frederick DT, Piris A, Cogdill AP, Cooper ZA, Lezcano C, Ferrone CR, et al. BRAF inhibition is associated with enhanced melanoma antigen expression and a more favorable tumor microenvironment in patients with metastatic melanoma. Clin Cancer Res 2013;19:1225–31.

[68] Liu C, Peng W, Xu C, Lou Y, Zhang M, Wargo JA, et al. BRAF inhibition increases tumor infiltration by T cells and enhances the antitumor activity of adoptive immunotherapy in mice. Clin Cancer Res 2013;19:393–403.